A 27-DAY PERIODICITY IN OUTER ZONE TRAPPED ELECTRON INTENSITIES

by

Donald J. Williams[1]

The Johns Hopkins University
Applied Physics Laboratory
Silver Spring, Maryland

[1] Now at Goddard Space Flight Center, Greenbelt, Maryland

[redacted]

ABSTRACT

Data from the polar orbiting satellite 1963 38C show the existence of a 27-day periodicity in the intensities of trapped, ≥ 280 kev and ≥ 1.2 Mev electrons for $L \geq 3.5$. This effect is seen for the four sequential solar rotations commencing October 6, 1963. The trapped energetic electron intensities are observed to undergo two large increases every 27 days and are shown to be intimately linked with the passage of the recently observed interplanetary magnetic field sector boundaries. It is also shown that these electron intensity increases are triggered by variations in the parameter β, the ratio of the directed solar wind kinetic energy density to the interplanetary magnetic field energy density. Equivalently, large variations in the Alfvén Mach number, M_A, are shown to be responsible for these trapped electron variations.

 [redacted]

INTRODUCTION

The possible existence of a 27-day periodicity in outer zone energetic trapped electron intensities was discussed in a recent study of the temporal behavior of such electrons as observed from the low altitude polar orbiting satellite, 1963 38C [Williams and Smith, 1965].

An additional but related observation in this study was that during periods of magnetic quiet, the outer zone trapped electron intensities exhibit a steady decay, implying that a quiescent solar wind does not supply fresh particles to the outer zone, at least not to high latitude ($L \geq 3$) low altitude trapping regions. Perturbations in the trapped electron population seem to occur mainly when the solar wind and/or interplanetary field direction changes.

The purpose of this note is to present and discuss data bearing on and extending the above observations. Trapped, energetic ($E_e \geq 280$ kev, ≥ 1.2 Mev) electron intensities have now been obtained through the first four solar rotations after the launch of 1963 38C. The data show a striking 27-day periodicity in that the trapped electron population throughout much of the outer zone ($L \geq 3.5$) undergoes an intensity increase twice every 27 days. Furthermore, this 27-day periodicity in the outer zone trapped electron intensities is intimately linked with the passage of the interplanetary magnetic field sectors reported by Ness and Wilcox [1965].

A further study by Wilcox and Ness [1965] has shown that variations of the interplanetary field strength, solar wind velocity and solar wind density are strongly coupled to the observed sector structure. These results are of interest in that they have allowed the observed variations in the trapped electron population to be linked directly to observed variations of a particular parameter in the interplanetary medium in the immediate vicinity of the magnetosphere, namely β, the ratio of the directed solar wind kinetic energy density to the magnetic field energy density.

The initial results confirming the existence of a 27-day periodicity in the trapped, energetic electron population in the outer zone at 1100 km have been presented previously (Williams, 1965). The present paper discusses these variations in much more detail and extends the analysis to include a phenomenological explanation of the observed electron behavior.

SATELLITE AND DETECTOR

The satellite 1963 38C and the detector of interest have been described in detail previously [Williams and Smith, 1965].

Briefly, the satellite 1963 38C was launched on September 28, 1963 into a nearly circular polar orbit having a 1140 km apogee, a 1067 km perigee, an 89.9° inclination and a 107.5 min. period. Just after launch the satellite orbital plane made an angle of $\sim 6^\circ$ with the noon-midnight meridian and was moving toward the noon-midnight meridian at the approximate rate of 1° per day due to the earth's motion about the sun. The satellite was magnetically aligned and displayed an oscillation of $\lesssim 6^\circ$ about the local line of force some three days after launch.

The experiment of interest is an integral electron spectrometer comprised of five, one millimeter thick, surface barrier solid state detectors. In this note, we shall only consider data from the two lower energy channels, namely the channels sensitive to electrons of energy $E_e \geq$ 280 kev and $E_e \geq$ 1.2 Mev respectively. A combination of discriminator levels and absorbing foils yields the particle and energy sensitivities shown in Table I. Monitoring an onboard proton spectrometer has shown that proton contamination in these outer zone electron data is negligible.

TABLE I

Pertinent Electron Spectrometer Characteristics

Detector	Energy Response (All energies in Mev)	
	Electrons	Protons
1	$E_e \geq 0.28$	$2.0 \leq E_p \leq 2.3$ and $E_p \geq 178$
2	$E_e \geq 1.2$	$14.4 \leq E_p \leq 14.5$ and $E_p \geq 179$

The spectrometer is oriented to look out normal to the satellite alignment axis. As the combination of the small detector look angle

(12.8° full angle) and the small resultant oscillation about the line of force ($\lesssim 6°$) is well removed from the local loss cone at 1100 km in the outer zone, the spectrometer measures the intensity of trapped electrons mirroring at, or very near, the point of observation.

Directional flux values (electrons per cm^2 sec ster) for the ≥ 280 kev and ≥ 1.2 Mev channels may be obtained to an accuracy of $< 50\%$ by multiplying the ≥ 280 kev **and** ≥ 1.2 Mev count rates by 500 and 1000 respectively.

As of October 1965, satellite 1963 38C was still in operation and transmitting data of high quality.

DATA

In an earlier study of the temporal behavior of trapped, ≥ 280 kev electrons at 1100 km on the sunlit hemisphere, [Williams and Smith, 1965] it was observed that electron intensity increases occurred during the time of the 27-day recurring increase in magnetic activity. However, only one solar rotation period was included in the analysis and no definite correlation with a 27-day period could be made.

We have now obtained the trapped, ≥ 280 kev and ≥ 1.2 Mev electron data at 1100 km on the sunlit hemisphere for the first four solar rotation periods after the launch of 1963 38C. The solar rotations analyzed are the four beginning October 6, 1963, November 2, 1963, November 29, 1963, and December 26, 1963.

The data have been reduced as intensity (counts per sec) versus time plots at half integral values of L from L = 3.0 through L = 6.0. The bulk of the data for these plots has been obtained from the APL receiving station at Silver Spring, Maryland, and the NASA receiving stations located at College, Alaska and Winkfield, England. In addition, NASA receiving stations located at Fort Meyers, Florida, East Grand Forks, Minnesota, Goldstone Lake, California and Woomera, Australia contributed approximately 10-20% of the data used in this analysis.

All these data have been plotted without regard to B value, yielding for example, a spread in B values at L = 5.0 for all the stations employed, of B = 0.32 gauss to B = 0.40 gauss. As noted previously [Williams and Smith, 1965] any variation in the data due to this range of B values seems to be far overshadowed by the temporal variations occurring throughout the outer zone. Furthermore, no sustained trend (longer than one or two days) in the count rate dependence on B was observed during the period under observation, i.e. in the observed B range, count rates were just as likely to be larger at high B values as at low B values.

The data points plotted are the result of a 5 point (~12 sec) averaging program. The central point of the group was within 0.03 earth radii of the desired L value at L = 6.0 and within 0.02 earth radii of the desired L value at L = 3.0. The 5 point averaging process introduced a total spread in L value of ±0.04 at L = 3.0 and $^{+.14}_{-.11}$ at L = 6.0. Again, the temporal variations being studied here are much larger than any variations which may be introduced by the above spread in L values in these high latitude, low altitude trapping regions.

We show in Figures 1 through 6, intensity (counts per sec) versus time plots for trapped, $\geq$ 280 kev and $\geq$ 1.2 Mev electrons on various L shells for the four consecutive solar rotations beginning October 6, 1963. Data are shown at L values of 3.0, 3.5, 4.5 and 5.0 for $\geq$ 280 kev electrons and L values of 4.5 and 5.0 for $\geq$ 1.2 Mev electrons. The remaining L shells studied support the discussion presented herein and have been omitted for reasons of brevity. Shown along with the electron data in Figures 1-6 are the 3 hour averages of K_p. The general correspondence between the electron intensities and magnetic activity is readily discernible.

During the latter two solar rotation periods shown in Figures 1-6, November 29 and December 26, 1963, the magnetometers aboard the NASA IMP-1 satellite were able to monitor the interplanetary magnetic field. For these two solar rotations plus the succeeding rotation beginning January 22, 1964, Ness and Wilcox [1965] have reported the existence of a regular longitudinal sector structure in the interplanetary field. The total longitudinal structure co-rotates with the sun and is separated into four sectors. In two of these sectors, each occupying about 2/7 of the total longitude, the field is directed away (+) from the sun. In the two remaining sectors, 2/7 and 1/7 of the total longitude, the field is directed toward (-) the sun. The sector boundaries are neutral sheets separating regions of oppositely directed field and produce, as they sweep past the earth, a rapidly changing transitional field configuration which may interact with the magnetosphere and its environs.

The average sector boundaries obtained by Ness and Wilcox [1965] for the three consecutive solar rotations beginning November 29, 1963 are included in the plots of Figures 1-6. We also include these average sector boundaries in the two preceding solar rotations, October 6 and November 2, 1963. It can be seen that the increase in trapped electron intensities observed near the beginning of a solar rotation for $L \gtrsim 3.5$, occurs at or just after the arrival of a sector boundary. It is interesting to note that for the rotations of November 2, November 29, and December 26, 1963, there is an additional particle increase at the arrival of the sector boundary located $\sim 180°$ from the initial particle increases. The passage of both of these boundaries produces a similar transitional field, i.e., the field changes from - to +. The latter portion of the October 6 rotation was obscured by two large storms and thus does not exhibit this effect. We shall at this point consider Figures 1-6 in more detail.

The trapped, $\gtrsim 280$ kev electron intensity at $L = 3.0$ for these solar rotations is shown in Figure 1 and no readily apparent 27-day variation can be observed. The only observed intensity changes are the sudden and large increases associated with sudden intense increases in magnetic activity occurring on October 24, 1963, October 29, 1963, and January 2, 1964. However, it is possible that the particle increase and magnetic activity of January 2, 1964 are associated with the passage of the sector boundary at ~2100 hrs on December 31, 1963. Nonetheless, particle increases at L = 3.0 seem to occur only during periods characteristized by intense magnetic activity. During the relatively quiet periods, the intensities show a steady decay right to the detector count rate threshold.

At L = 3.5 (Figure 2) a 27-day periodicity is just discernible. Note that the size of the increase at L = 3.5 is such that it is not noticeable in the November 2, 1963 rotation due to the enhanced intensities reached during the storms of October 24 and 29, 1963. Thus the 27-day intensity variations being presented here may be observable only during the quiescent conditions of solar minimum and may be negligible effects during the enhanced activity near solar maximum.

No 27-day periodicity was observable at L = 3.5 for the intensities of trapped, ≥ 1.2 Mev electrons.

Figures 3, 4, 5, and 6 clearly show the 27-day periodicity present in trapped, energetic electron intensities in the outer zone. In addition to the large intensity increase occurring at the arrival of the first 2/7 sector, there is now observed an additional increase at the arrival of the next sector producing the same transitional field (- to +). Both energies observed, $E_e \geq 280$ kev and ≥ 1.2 Mev, behave in essentially the same manner with the main difference being that the ≥ 280 kev electrons attain peak intensities a few days before the ≥ 1.2 Mev electrons.

Note that the initial electron intensity increase in the November 29, 1963 rotation occurs 1.5 to 2 days before the arrival of the sector boundary shown at 2100 hours on December 4, 1963. This can be explained by recalling that the sector boundary arrival times shown in Figures 1-6 are the average values presented by Ness and Wilcox (1965). However, as mentioned by Ness and Wilcox (1965) and amplified by Wilcox and Ness (1965), the November 29, 1963 rotation is somewhat of an exception to their proposed sector structure in that the arrival of the first 2/7 boundary took place at 21xx hours on December 2, 1963 rather than at the expected time of 2100 hours on December 4, 1963. This earlier arrival was explained by Wilcox and Ness (1965) as due to a higher observed average solar wind velocity on December 2, 1963 than during the remaining 3 solar rotations. It is seen that the actual boundary arrival time of 21xx hours on December 2, 1963 agrees remarkably well with the observed electron intensity increases.

Concurrent with the boundary arrival at 21xx hours on December 2, 1963 was the start of a sudden commencement (sc) magnetic storm at

2116 hours [Lincoln, 1964]. As the trapped electron intensity increase occurring at the beginning of December, 1963 could be associated with this sc magnetic storm, we have listed in Table 2, all sc's for the period shown in Figures 1-6, October 6, 1963 through January 21, 1964 [Lincoln, 1964 and 1965]. Comparison of Table 2 with Figures 1-6 shows that electron increases occur at boundary passages where no sc's are reported and thus, while they may themselves be associated with the sector boundaries, the sc's are not the cause of the periodic electron increases. In fact, the general correlation between the Kp index and trapped electron intensities probably only exists because both parameters are affected by the solar wind-magnetospheric interaction, i.e., rather than a cause and effect correlation, it is a correlation linking two effects of a common cause, the solar wind-magnetospheric interaction.

TABLE 2

Sudden Commencements Given by
Ten or More Stations

Date	UT (hours)
Oct. 29, 1963	1359
Nov. 17, 1963	0903
Nov. 22, 1963	1547
Dec. 1, 1963	2226
Dec. 2, 1963	2116
Dec. 28, 1963	0756
Jan. 1, 1964	1148

Thus we see that in general, throughout the outer zone ($L \geq 3.5$), the trapped, energetic electron population exhibits a clear 27-day periodicity in that the intensity of these electrons increases twice every 27-days. These increases are strongly correlated to the passage of the interplanetary field sector boundaries. Further, it is the arrival of the sector boundaries defining a field toward sun (-) to field away from sun (+) transition in the vicinity of the magnetosphere, which triggers the major electron intensity increases. It is possible however, to see some evidence for changes in the electron intensities near the arrival of the remaining boundaries, e.g. see the January 8, 1963 sector boundary in Figures 3, 4, 5, and 6. This particular variation seems more enhanced at yet higher L values. Nevertheless, the major 27-day electron intensity increases throughout the outer zone as observed at 1100 km are associated with the - to + transition.

DISCUSSION

These results show the existence of a distinct 27-day periodicity in the outer zone trapped electron intensities. They further indicate that the major 27-day electron increases are associated with the arrival of the sector boundaries producing a - to + interplanetary field transition in the vicinity of the magnetosphere. The remaining two sector boundaries (defining the + to - transition) produce much smaller, and possibly no, changes in the trapped electron population. In this section we present a phenomenological explanation for the above behavior.

It is a widespread assumption that the primary energy source for magnetic storms, auroras, trapped radiation variations etc. is the solar wind. The principle mechanisms proposed for coupling the solar wind energy into the magnetosphere are a viscous interaction between the solar wind and the magnetosphere (Axford and Hines, 1961; Axford, 1964), an interconnection model in which interplanetary field lines are able to connect to high latitude field lines of the earth's magnetic field (Dungey, 1961) and the generation of hydromagnetic waves by the response of the magnetospheric cavity to a changing interplanetary magnetic field direction (Dessler and Walters, 1964).

The explanation of sudden commencement rise times (Dessler et al, 1960) and the observation of an extended geomagnetic tail (Ness, 1965) can be regarded as evidence consistent with the viscous interaction hypothesis (Axford and Hines, 1961). While under considerable harassment, the interconnection hypothesis (Dungey, 1961) has received some support in the recent findings of Fairfield and Cahill (1965) where they obtain a correlation of north to south transitions in the interplanetary field direction with increased magnetic activity.

Consideration of the effect of the presence of a weak interplanetary magnetic field on the behavior of the solar wind in the vicinity of the magnetosphere led to the prediction of the existence of a shock front a few earth radii in the solar direction from the magnetospheric boundary

(Axford, 1962; Kellogg, 1962). Such a shock front in agreement with the predictions, has been observed by the magnetometers aboard the NASA IMP-1 satellite (Ness et al, 1964).

Walters [1964] has further argued that an additional effect of an oblique interplanetary field in the ecliptic plane is to cause the axis of symmetry of the magnetosphere to be shifted several degrees from the earth-sun line, as if the solar wind came from an apparent direction some several degrees west of the sun. This is due to the interplanetary field causing an easterly deflection of the radially expanding solar wind as it traverses the shock front mentioned above. The amount of deflection is dependent on the angle between the interplanetary field and the direction of solar wind flow, ψ, and on the ratio of the directed solar wind kinetic energy density to the magnetic energy density, β. The interplanetary magnetic field has been observed by Ness and Wilcox [1965], to lie, on the average, in the ecliptic plane and to make an angle of about 45° to the earth-sun line in the vicinity of the magnetosphere, forming a picture consistent with the Archimedean spiral angle predicted by Parker [1958].

Using the results of Walters (1964), Dessler and Walters (1964) have presented a model in which the magnetospheric cavity will oscillate to and fro in concert with variations in the direction of the interplanetary magnetic field and will thereby couple solar wind energy to the magnetospheric cavity via the subsequent generation of hydromagnetic waves.

With the above brief discussion in mind, we shall proceed to a consideration of the results presented in the last section. An explanation is required for the fact that there appear to be only two electron intensity increases per 27 days and that these increases are associated with the passage of the sector boundaries defining a - to + transition. If it were chiefly variations in the interplanetary field direction which coupled energy into the magnetosphere (Dessler and Walters, 1964), then one would expect four increases every 27 days, resulting from the observational fact (Ness and Wilcox, 1965) that there are four co-rotating sector boundaries which separate regions of oppositely directed field.

Wilcox and Ness [1965] have presented the variation of the interplanetary magnetic field strength, the solar wind velocity and the solar wind density as a function of position, in time, within a 2/7 sector. Such correlations were also performed for the solar wind flux, geomagnetic activity and the Deep River neutron monitor for both the + and - sectors. All parameters considered showed a definite and consistent variation as a function of position within the sector.

To further understand the trapped electron intensity increases presented herein, we have used the data of Wilcox and Ness (1965) for the 2/7 sectors, and have computed and plotted the directed solar wind kinetic energy density, $1/2\ mnV^2$, the magnetic field energy density, $B^2/8\pi$, and their ratio, $\beta = (4\pi/B^2)mnV^2$. Here m = proton mass, n = solar wind number density, V = solar wind velocity and B = magnitude of the interplanetary magnetic field. These computations were performed separately for the + and - sectors.

The results for the directed solar wind kinetic energy density and the magnetic energy density are shown in Figure 7. The ratio, β, is shown in Figure 8. Here, in Figures 7 and 8, we have plotted these parameters as a function of position, in time, within a sector but have placed the sectors in series so as to show the variation throughout the three consecutive 2/7 sectors.

The remarkable feature of the variation of β (Figure 8) is that it undergoes a large variation at the boundary defining the - to + transition, which is where the trapped electron increases occur. At the + to - transition boundary, β remains relatively steady as do the trapped electron intensities.

This indicates that the primary trigger for the trapped electron intensity variations presented here, is large variations in the ratio of the directed solar wind energy density to the magnetic energy density, β. To use a fluid analogy, we note that the Alfvén speed is given by

$$V_A^2 = \frac{B^2}{4\pi\rho}$$

where ρ = mass density. This yields

$$\beta = \frac{4\pi\rho V^2}{B^2} = \frac{V^2}{V_A^2} = M_A^2$$

where M_A is the Alfvén Mach number. A scale of $M_A = \sqrt{\beta}$ is included in Figure 8.

Alternatively, we thus see that the trapped electron intensity increases occur only when there are large changes in the Alfvén Mach number. In the present case the solar wind is highly supersonic and strongly shocked during quiescent times and changes to an extremely supersonic and very strongly shocked condition at the boundary defining the - to + transition.

We note that the above arguments and conclusions are supported by the observed behavior of M_A (or β) within the 2/7 sectors only, Figures 7 and 8. Only two 1/7 sectors were observed and due to the consequent poor statistics were not shown in the superposed epoch analysis (Ness and Wilcox, private communication). However these authors have kindly made the 1/7 sector data available so that the above conclusions could be checked in general.

There were only two usable examples of a 1/7 sector observed by the magnetometers aboard IMP-1. Furthermore, the beginning and ending times of these sectors were obscured by IMP-1 being near perigee. Because of these effects and the existing poor statistics we show separately in Figure 9, both of these 1/7 sectors plotted in series with the data of Figure 8. Note that only the Alfven Mach number, M_A , is shown. The shaded areas indicate the time interval during which the 1/7 sector boundary occurred – the exact time not being known due to IMP-1 being at perigee. The circled plus signs, $\oplus$, shown near the beginning of the first 2/7 sector, are the actual individual points obtained after it was known that the 1/7 sector boundary had passed. These points are included to show agreement with the generally low average values obtained for the same relative position within the + 2/7 sectors.

Again we see from Figure 9, albeit with more scatter in the data, that M_A undergoes large variations at the sector boundary defining the - to + interplanetary field transition, correlating with the outer zone electron intensity increases. The + to - transition is seen to produce far less variation in M_A and in outer zone electron intensities.

The inclusion of the 1/7 sectors further supports our conclusions that the trapped electron intensity increases presented herein occur only when there are large changes in the Alfvén Mach number, M_A.

It is important to note that there is little change in β at the + to - transition boundary and correspondingly little variation in the trapped electron intensities, although there is a large change in the interplanetary field direction. This seems to contradict the arguments of Walters (1964) and Dessler and Walters (1964) concerning the effects of an oblique interplanetary magnetic field on the tilt of the magnetosphere and the subsequent hydromagnetic energy coupling mechanism proposed. However for such highly supersonic behavior as obtained for the period under observation here, $40 \lesssim \beta \lesssim 240$, the effective tilting of the magnetospheric axis will be very small (Walters, 1964) and subsequent magnetospheric twitching due to a changing interplanetary field direction may be inconsequential. This argument is supported by the observation of Ness et al. (1964) that during this period the tilt of the magnetospheric axis away from the earth-sun line was $\sim 5^{\circ}$ – a result comparable to the aberation expected, under the observed solar wind conditions, due to the earth's motion about the sun.

SUMMARY AND CONCLUSIONS

Evidence for a 27-day variation in the intensities of trapped, energetic ($E_e \geq 280$ kev and ≥ 1.2 Mev) electrons in the outer zone at 1100 km has been presented. It was seen that the intensities of these electrons throughout much of the outer zone ($L \geq 3.5$) underwent a significant increase twice every 27 days. The spatial and energy dependence of this effect was also indicated.

It was further seen that these intensity increases occurred at or just after the passage of the interplanetary sector boundaries (Ness and Wilcox, 1965) which defined the - to + field transitions in the vicinity of the magnetosphere (the minus sign signifies field toward sun and the plus sign signifies field away from sun). The passage of the remaining two sector boundaries, defining the + to - field transition, produced a much smaller, and possibly no, variation in the trapped electron intensities.

It was then shown, using the data of Wilcox and Ness, 1965, that the primary trigger (or solar wind-magnetospheric energy coupling mechanism) for these trapped electron increases was large variations in β, the ratio of the directed solar wind kinetic energy density to the magnetic energy density, or equivalently, large variations in the Alfvĕn Mach number of the solar wind, M_A. This supports the viscous interaction, energy coupling model of Axford and Hines (1961), at least for the highly supersonic conditions as existed during the period under study.

These results clearly display the intimate connection between the magnetospheric trapping regions and conditions in the interplanetary medium. They also emphasize the interesting fact that these mild perturbations (compared to conditions near solar maximum) are able to significantly alter the relativistic electron population deep in the magnetosphere ($L \geq 3.5$).

ACKNOWLEDGMENTS

I acknowledge and deeply appreciate the contribution to this study, of the previously unpublished 1/7 sector data by Drs. J. M. Wilcox and

N. F. Ness. Discussions with Dr. N. F. Ness of these results and their relevance are also appreciated.

This work was supported in part by the Bureau of Naval Weapons, Department of the Navy, under contract NOw 62-0604-c and in part by a National Aeronautics and Space Administration Grant.

References

Axford, I. W., Viscous interaction between the solar wind and the Earth's magnetosphere, Planet. Space Sci., 12, 45-53, 1964.

Axford, I. W., The interaction between the solar wind and the Earth's magnetosphere, J. Geophys. Res., 67, 3791-3796, 1962.

Axford, I. W., and C. O. Hines, A unifying theory of high-latitude geophysical phenomena and geomagnetic storms, Can. J. Phys., 39, 1433-1464, 1961.

Dessler, A. J., W. E. Francis, and E. N. Parker, Geomagnetic storm sudden-commencement rise times, J. Geophys. Res., 65, 2715-2719, 1960.

Dessler, A. J., and G. K. Walters, Hydromagnetic coupling between solar wind and magnetosphere, Planet. Space Sci., 12, 227-234, 1964.

Dungey, J. W., Interplanetary magnetic field and the auroral zones, Phys. Rev. Letters, 6, 47-48, 1961.

Fairfield, D. H., and L. J. Cahill, The interplanetary magnetic field and polar magnetic disturbances, Univ. of New Hampshire Dept. of Physics pub. UNH-65-1, Durham, New Hampshire, 1965.

Kellogg, P. J., Flow of plasma around the Earth, J. Geophys. Rev., 67, 3805-3811, 1962.

Lincoln, J. V., Geomagnetic and solar data, J. Geophys. Res., 70, 1227-1229, 1965.

Lincoln, J. V., Geomagnetic and solar data, J. Geophys. Res., 69, 3283-3287, 1964.

Ness, N. F., The Earth's magnetic tail, J. Geophys. Res., 70, 2989-3005, 1965.

Ness, N. F., C. S. Scearce, and J. B. Seek, Initial results of the IMP-1 magnetic field experiment, J. Geophys. Res., 69, 3531-3569, 1964.

Ness, N. F., and J. M. Wilcox, Sector structure of the quiet interplanetary magnetic field, Science, 148, 1592-1594, 1965.

Parker, E. N., Dynamics of the interplanetary gas and magnetic fields, Ap. J., 128, 664-676, 1958.

Walters, G. K., Effect of oblique interplanetary magnetic field on shape and behavior of the magnetosphere, J. Geophys. Res., 69, 1769-1783.

Wilcox, J. M., and N. F. Ness, A quasi-stationary co-rotating structure in the interplanetary medium, J. Geophys. Res., 70, Dec. 1, 1965.

Williams, D. J., Outer zone electrons, presented at the Advanced Study Institute, "Radiation trapped in the Earth's Magnetic Field," Aug. 16 - Sep. 3, 1965, Bergen, Norway.

Williams, D. J., and A. M. Smith, Daytime trapped electron intensities at high latitudes at 1100 kilometers, J. Geophys. Res., 70, 541-556, 1965.

Figure Captions

Figure 1: Trapped electron intensities for the four consecutive solar rotations beginning October 6, 1963. Data are for $E_e \geq 280$ kev, L = 3.0 and 1100 km. The occurrence of the interplanetary magnetic field sector boundaries is shown, + = field away from sun, - = field toward sun (Ness and Wilcox, 1965). A plot of the 3 hour average Kp values is also included.

Figure 2: Same as Figure 1, L = 3.5.

Figure 3: Same as Figure 1, L = 4.5.

Figure 4: Same as Figure 1, L = 5.0.

Figure 5: Same as Figure 1, L = 4.5, $E_e \geq 1.2$ Mev.

Figure 6: Same as Figure 1, L = 5.0, $E_e \geq 1.2$ Mev.

Figure 7: Plot showing behavior of the directed solar wind kinetic energy density, $\frac{1}{2} \rho v^2$, and the magnetic field energy density $B^2/8\pi$, during the time interval occupied by three consecutive 2/7 sectors. Sector boundaries are marked as heavy vertical dashes and time in days is recycled at the beginning of each sector.

Figure 8: Plot showing the behavior of β, the ratio of the directed solar wind kinetic energy density to the magnetic field energy density, during the time interval defined by three consecutive 2/7 sectors. Note that the large variations in β seem to occur only at the boundary defining the - to + interplanetary field transition. A scale of the Alfvén Mach number, $M_A = \sqrt{\beta}$, is also included.

Figure 9: Plot showing the behavior of the Alfvén Mach number, M_A, for a 27 day period defined by a 1/7 sector followed by three consecutive 2/7 sectors. The additional data of the 1/7 sectors further support the observation that large variations in M_A seem to be associated with the sector boundaries defining the - to + interplanetary field transition. This correlates well with the observed trapped electron intensity increases. The slightly variable length in the time scale of the above plots is due to the uncertainty inherent in the beginning and ending times of the 1/7 sectors. The shaded areas show these uncertainties.

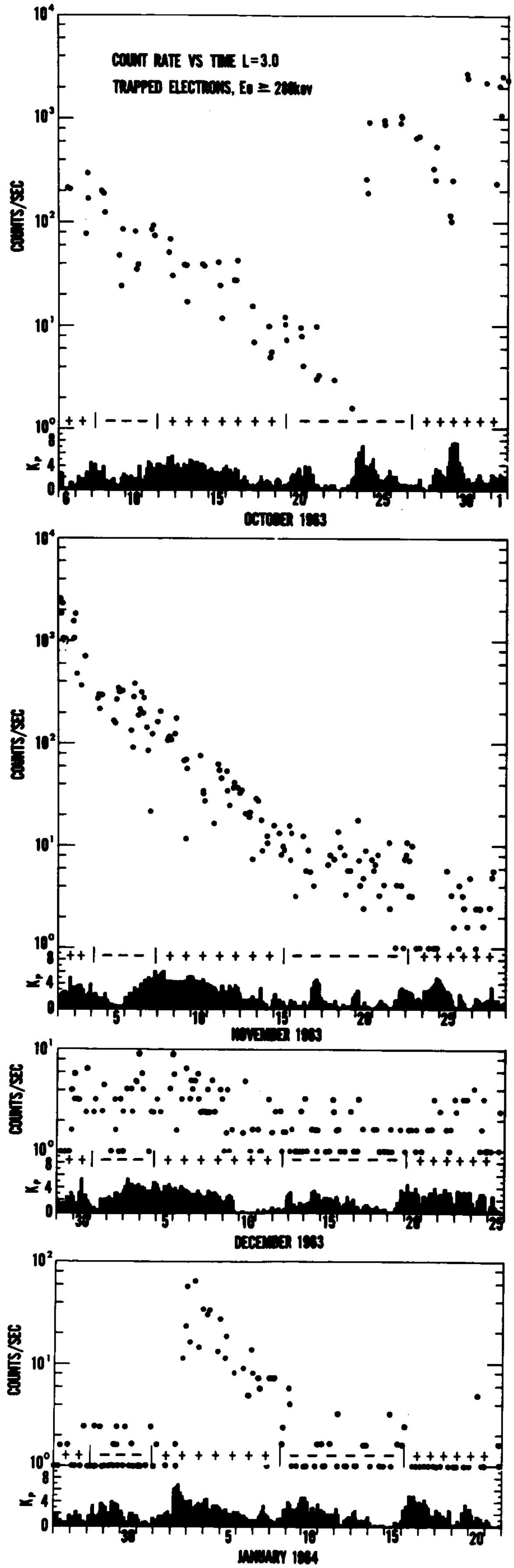

COUNT RATE VS TIME L=3.0
TRAPPED ELECTRONS, Eo ≥ 280kev
COUNTS/SEC
K_p
OCTOBER 1963
NOVEMBER 1963
DECEMBER 1963
JANUARY 1964

Figure 1

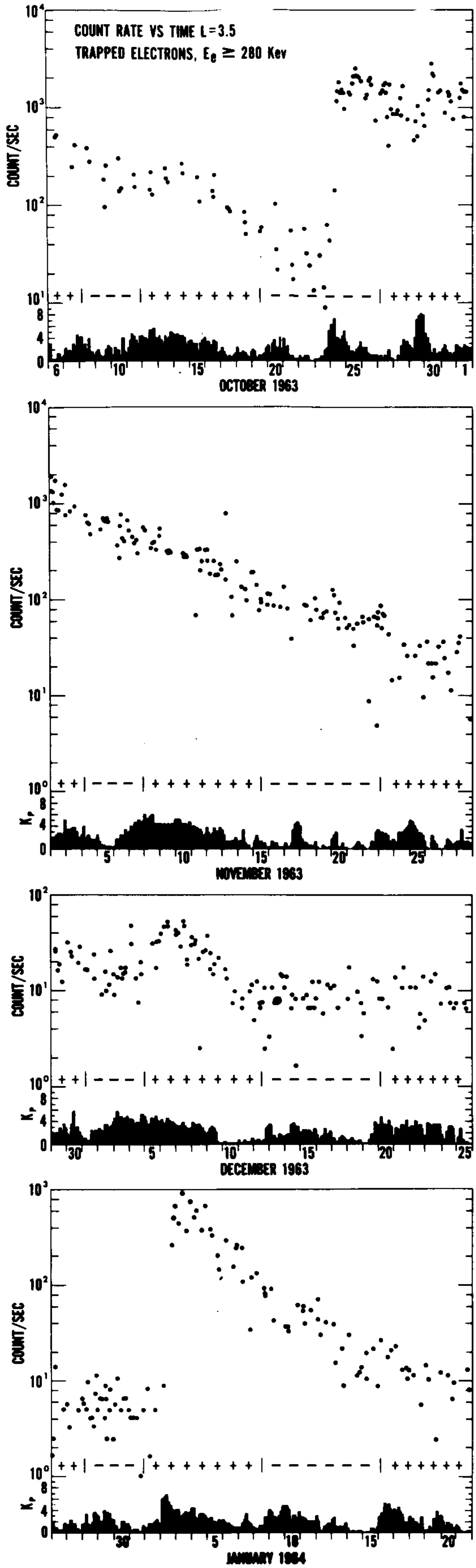
COUNT RATE VS TIME L=3.5
TRAPPED ELECTRONS, $E_e \geq 280$ Kev
COUNT/SEC
OCTOBER 1963
NOVEMBER 1963
DECEMBER 1963
JANUARY 1964
K_p

Figure 2

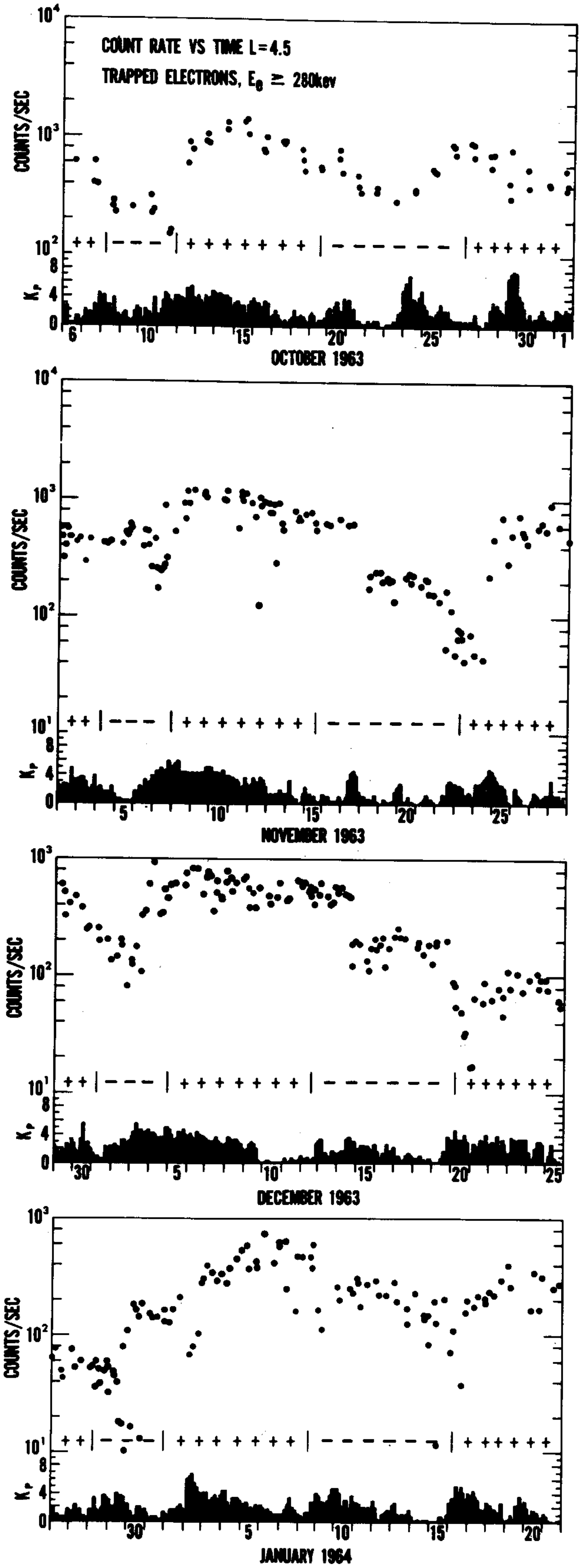
COUNT RATE VS TIME L=4.5
TRAPPED ELECTRONS, $E_\beta \geq 280$kev
COUNTS/SEC
K_p
OCTOBER 1963
NOVEMBER 1963
DECEMBER 1963
JANUARY 1964

Figure 3

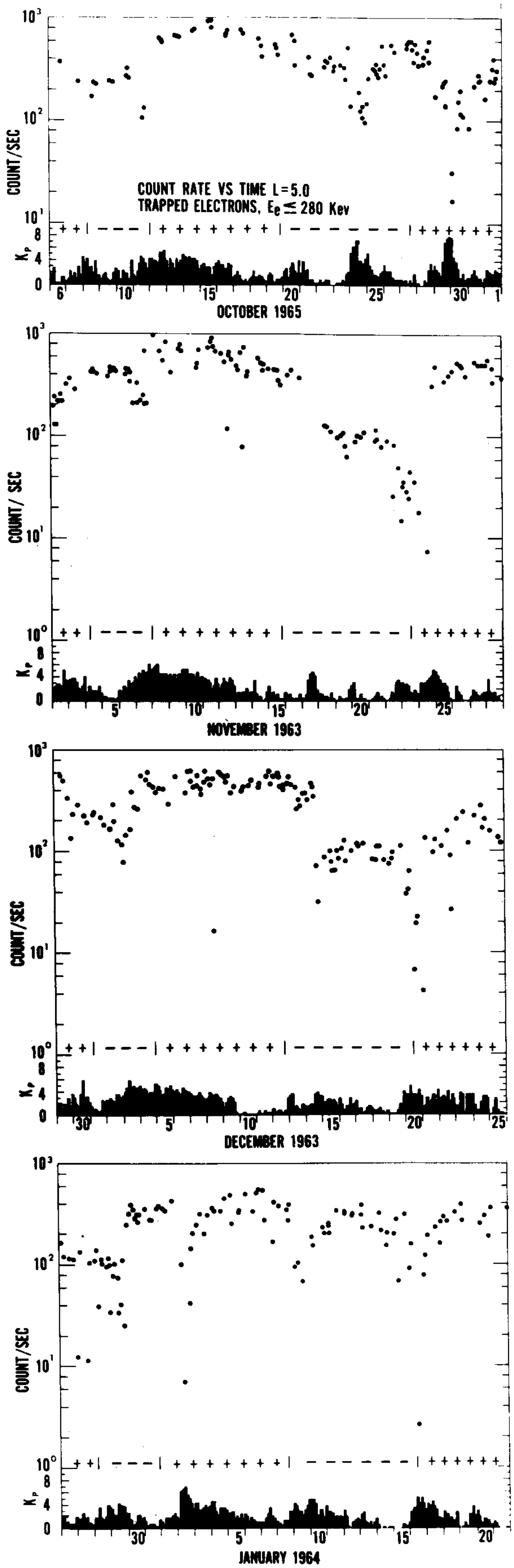

COUNT RATE VS TIME L=5.0
TRAPPED ELECTRONS, $E_e \leq 280$ Kev
COUNT/SEC
K_p
OCTOBER 1965
NOVEMBER 1963
DECEMBER 1963
JANUARY 1964

Figure 4

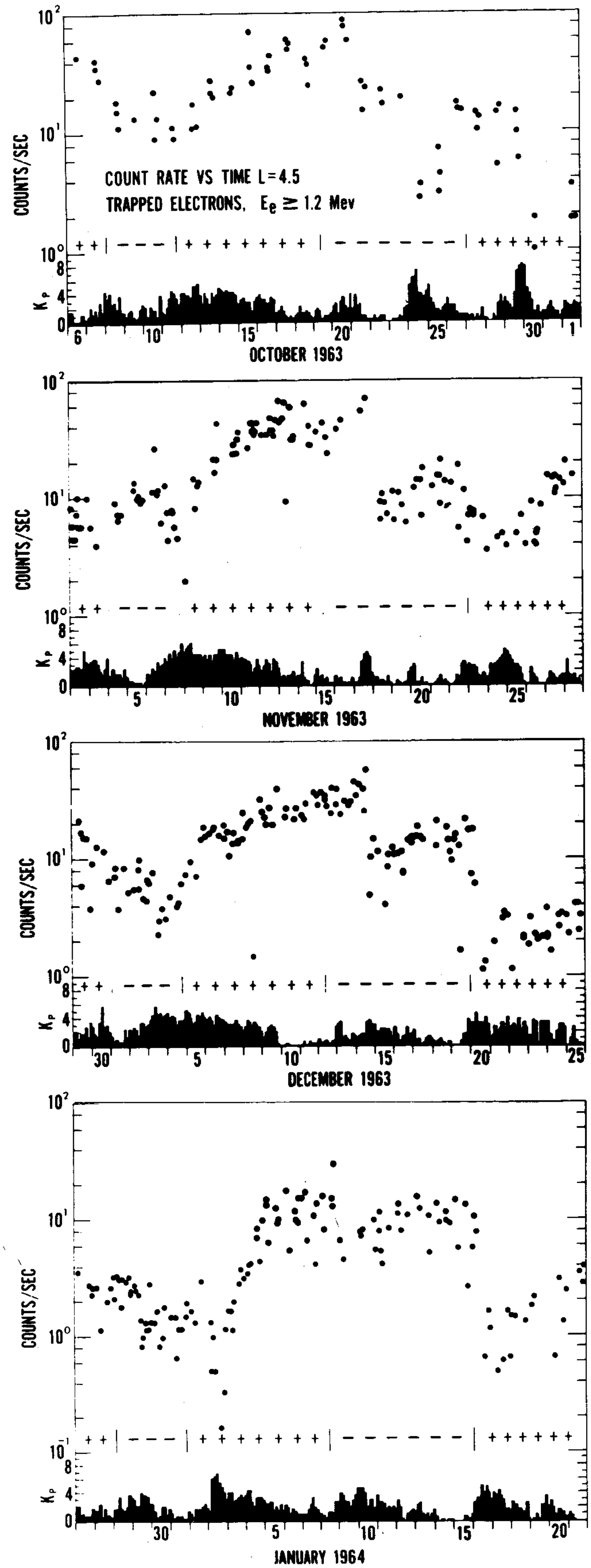
COUNT RATE VS TIME L=4.5
TRAPPED ELECTRONS, $E_e \geq 1.2$ Mev
COUNTS/SEC
K_p
OCTOBER 1963
NOVEMBER 1963
DECEMBER 1963
JANUARY 1964

Figure 5

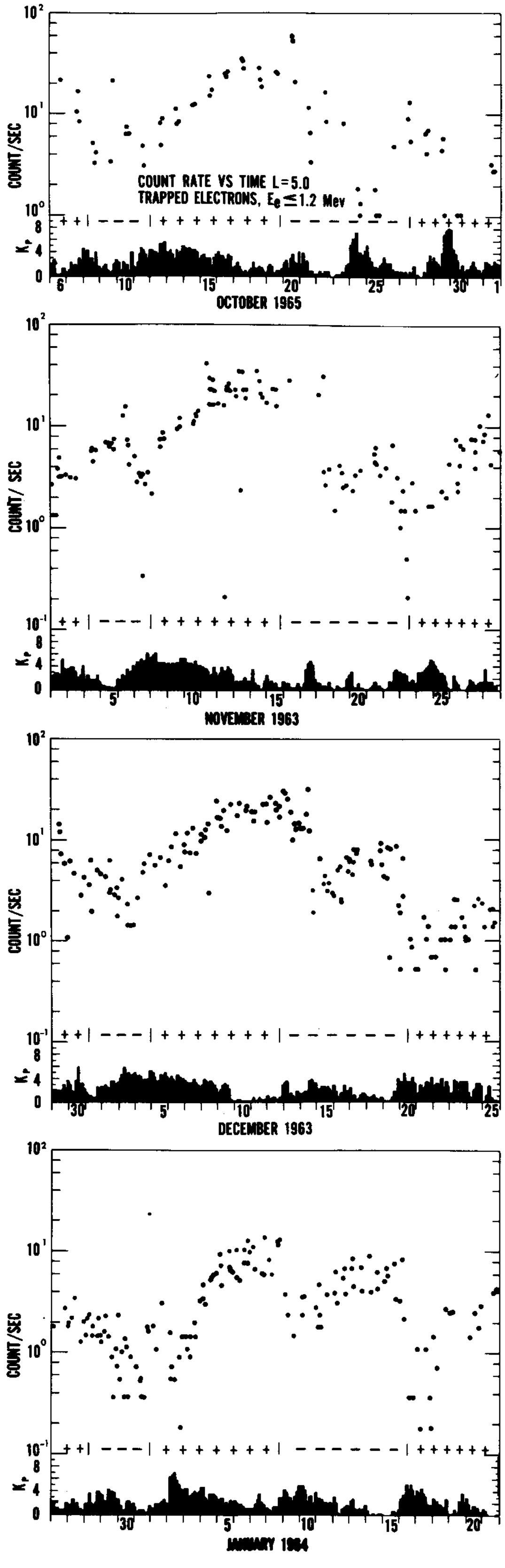
COUNT RATE VS TIME L=5.0
TRAPPED ELECTRONS, $E_e \leq 1.2$ Mev
COUNT/SEC
K_p
OCTOBER 1965
NOVEMBER 1963
DECEMBER 1963
JANUARY 1964

Figure 6

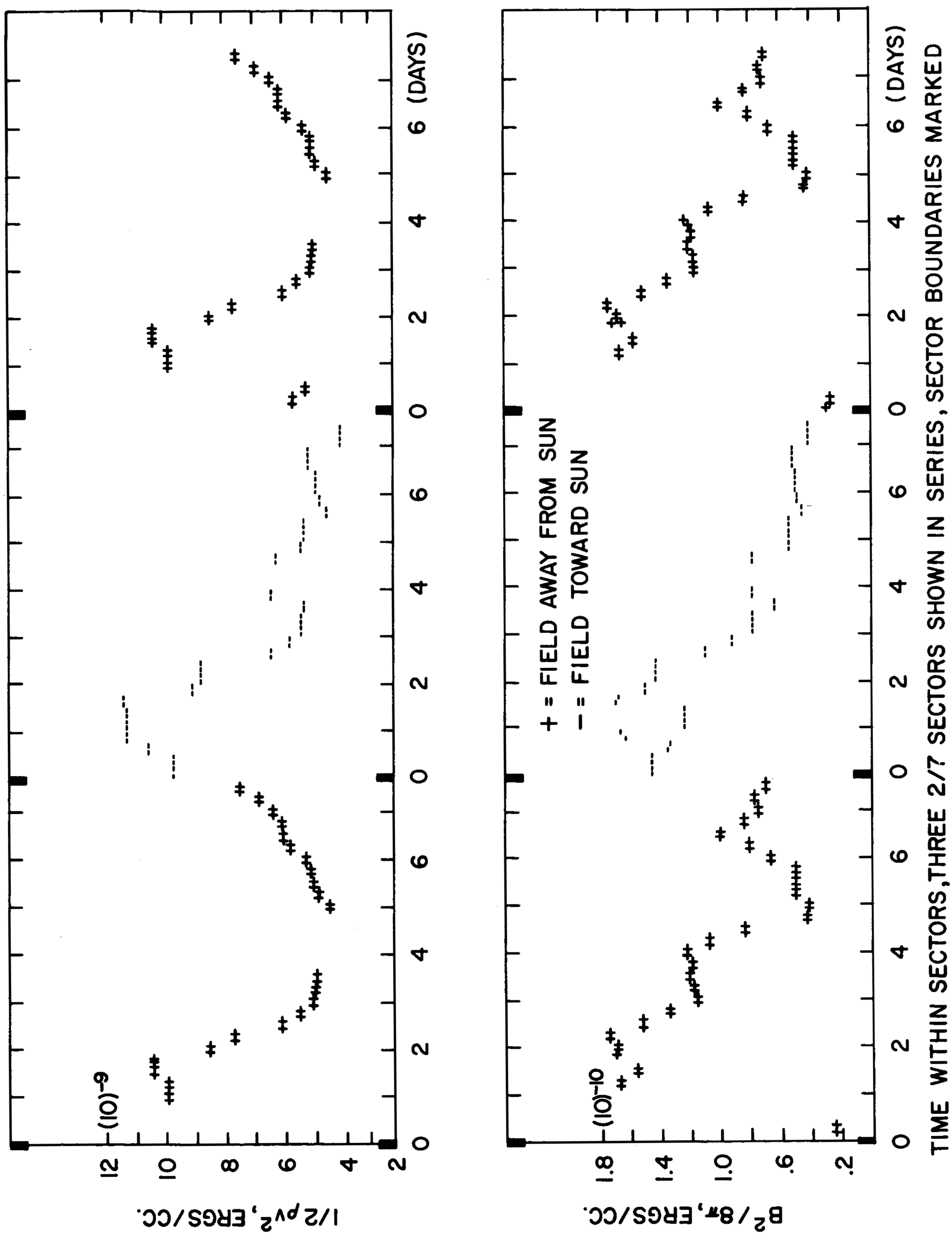
TIME WITHIN SECTORS, THREE 2/7 SECTORS SHOWN IN SERIES, SECTOR BOUNDARIES MARKED
(DAYS)
+ = FIELD AWAY FROM SUN
− = FIELD TOWARD SUN
1/2 ρv², ERGS/CC.
(10)⁻⁹
B²/8π, ERGS/CC.
(10)⁻¹⁰

Figure 7

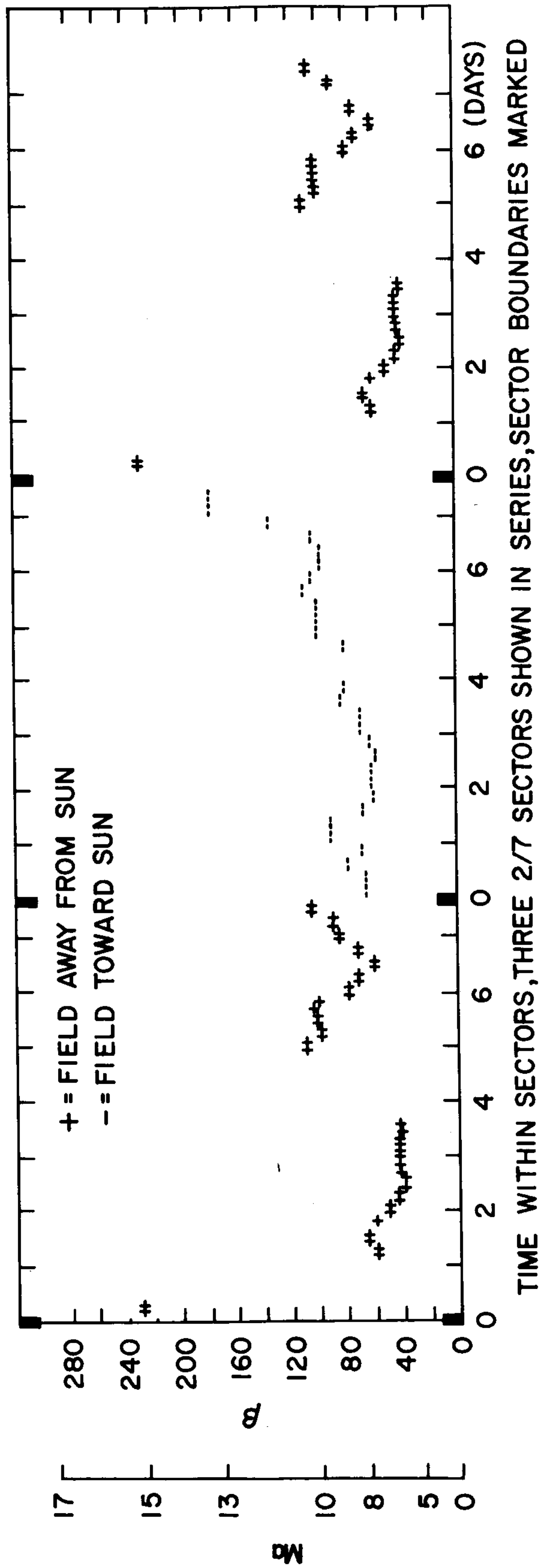
+ = FIELD AWAY FROM SUN
- = FIELD TOWARD SUN
TIME WITHIN SECTORS, THREE 2/7 SECTORS SHOWN IN SERIES, SECTOR BOUNDARIES MARKED
(DAYS)
β
Mα

Figure 8

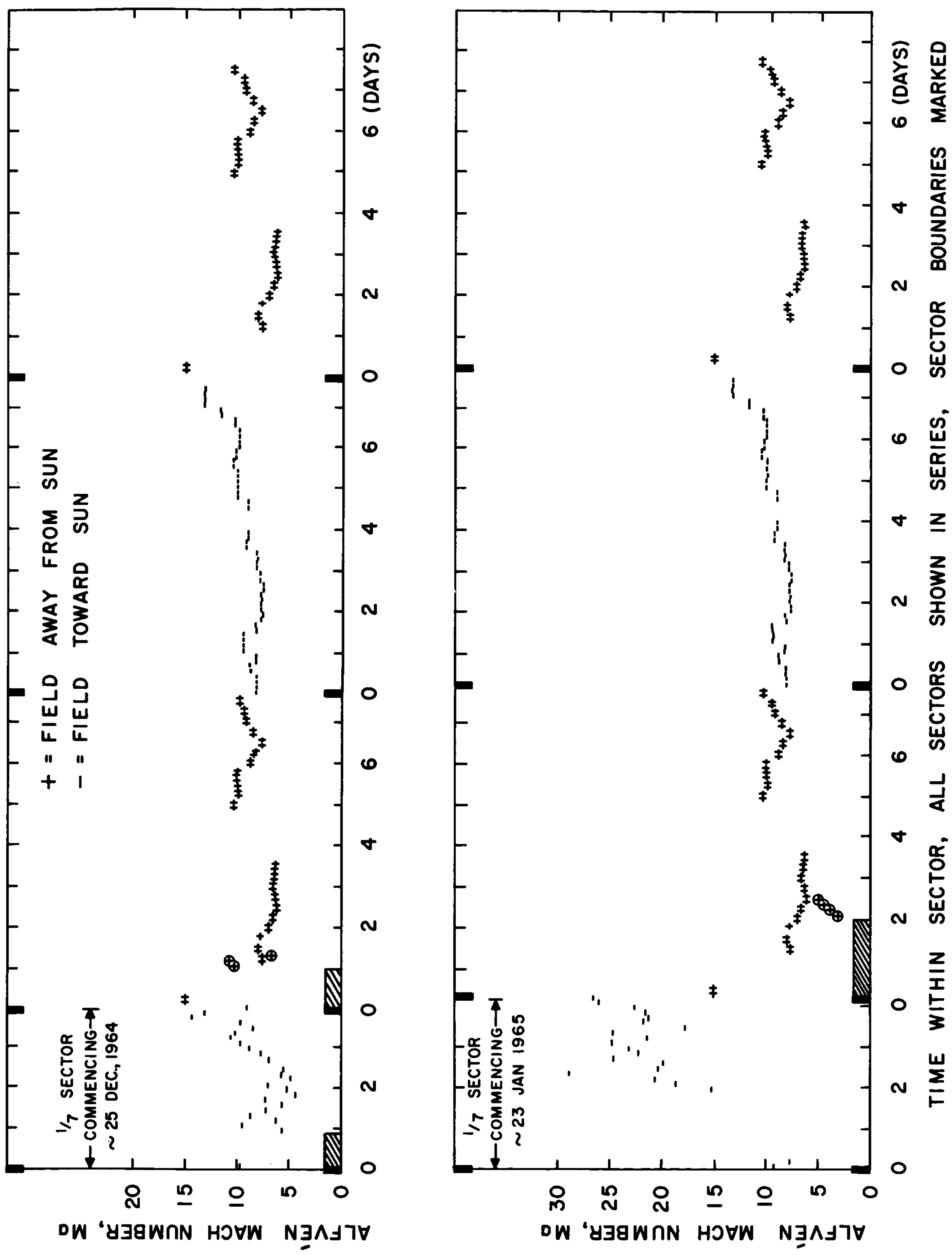
+ = FIELD AWAY FROM SUN
− = FIELD TOWARD SUN
1/7 SECTOR COMMENCING ~25 DEC., 1964
1/7 SECTOR COMMENCING ~23 JAN 1965
ALFVÉN MACH NUMBER, Ma
6 (DAYS)
TIME WITHIN SECTOR, ALL SECTORS SHOWN IN SERIES, SECTOR BOUNDARIES MARKED

Figure 9